CHIN. PHYS. LETT. Vol. 38, No. 8 (2021) 089101

Site-Selective Magnetic Moment Collapse in Compressed Fe_5O_6

Qiao-Ying Qin(秦巧英)[1†], Ai-Qin Yang(杨爱芹)[1†], Xiang-Ru Tao(陶相如)[1], Liu-Xiang Yang(杨留响)[2], Hui-Yang Gou(缑慧阳)[2*], and Peng Zhang(张朋)[1*]

[1]*MOE Key Laboratory for Nonequilibrium Synthesis and Modulation of Condensed Matter, School of Physics, Xi'an Jiaotong University, Xi'an 710049, China*

[2]*Center for High Pressure Science and Technology Advanced Research, Beijing 100094, China*

(Received 4 May 2021; accepted 7 June 2021; published online 2 August 2021)

Iron oxide is one of the most important components in the Earth's mantle. The recent discovery of the stable presence of Fe_5O_6 in the Earth's mantle environment has stimulated significant interests in understanding of this new category of iron oxides. We report the electronic structure and magnetic properties of Fe_5O_6 calculated by the density functional theory plus dynamic mean field theory (DFT + DMFT) approach. Our calculations indicate that Fe_5O_6 is a conductor at ambient pressure with dominant Fe-3*d* density of states at the Fermi level. The magnetic moments of iron atoms at three non-equivalent crystallographic sites in Fe_5O_6 collapse at significantly different rates under pressure. This site-selective collapse of magnetic moments originates from the shifting of energy levels and the consequent charge transfer among the Fe-3*d* orbits when Fe_5O_6 is being compressed. Our simulations suggest that there could be high conductivity and volume contraction in Fe_5O_6 at high pressure, which may induce anomalous features in seismic velocity, energy exchange, and mass distribution in the deep interior of the Earth.

DOI: 10.1088/0256-307X/38/8/089101

Iron oxide is one of the most abundant components in the Earth's mantle, accounting for about 7.5% of the total mass of the Earth.[1,2] The temperature in the Earth's mantle ranges from 500 K to 3000 K and the pressure ranges from 20 GPa to 140 GPa. The behavior of iron oxide at high temperature and high pressure is essential for our understanding of the evolution of the Earth's interior.[3] Under ambient conditions, there are three known forms of iron oxides: wüstite (FeO), hematite (Fe_2O_3) and magnetite (Fe_3O_4).[4] Iron oxides have also been widely used in industry,[5–9] therefore they have attracted extensive interest in scientific communities.

Recently, a series of new iron oxides were identified at high pressures and high temperatures, including FeO_2,[10,11] Fe_4O_5,[12] Fe_5O_6,[13] Fe_5O_7,[14] Fe_7O_9[15] and $Fe_{13}O_{19}$.[16] Among these iron oxides, Fe_5O_6 is synthesized by iron and hematite fine powder at ratio ($Fe + 2Fe_2O_3 = Fe_5O_6$) in a diamond anvil chamber at pressure ranges from 10 GPa to 20 GPa and temperature at about 2000 K.[13] This experiment indicates that the crystal structure of Fe_5O_6 is orthorhombic (*Cmcm* space group) with lattice parameters of $a = 5.319579$ bohr, $b = 18.510432$ bohr, $c = 28.367432$ bohr at 11.4 GPa.[13] There are three non-equivalent iron atoms and four unequal oxygen atoms in Fe_5O_6. As shown in Fig. 1, the iron atom at site-4*c* (Fe1) and the surrounding six oxygen atoms form a triangular prism, in contrast the other two iron atoms at site-8*f*1 (Fe2) and site-8*f*2 (Fe3) with their surrounding six oxygen atoms form octahedra, respectively. Since Fe_5O_6 is phase stable under high temperatures and high pressures, it is expected to be an important candidate material in the interior of the Earth, along with the other iron oxides. An experiment by Hikosaka *et al.* shows that Fe_5O_6 will decompose into $FeO+Fe_4O_5$ below 10 GPa and will decompose into $2FeO + Fe_3O_4$ above 38 GPa.[17] A recent experiment by Ovsyannikov *et al.* indicates the coexistence of the Verwey-type charge-ordering and the dimerization of iron atoms below 275 K,[18] where they find that such charge ordering can be tuned by the Fe–Fe distance of the octahedral chain in Fe_5O_6. They further suggest that Fe_5O_6 could be used for memory devices or switches by controlling its charge ordering around room temperature.

The discovery of energetically stable Fe_5O_6 at high pressure has opened up the possibility that it could be new candidate for the Earth's mantle material. Unfortunately, so far experimental and theoretical research of Fe_5O_6 at the Earth's mantle conditions has been very limited.[13,17,18] In this Letter, we use the DFT + DMFT[19] method to calculate the electronic and the magnetic properties of paramagnetic Fe_5O_6 at high pressures and high temperatures. Our calculation proves that Fe_5O_6 is a metal with site-dependent

Supported by the National Natural Science Foundation of China (Grant Nos. 11604255 and U1930401), and the Natural Science Basic Research Program of Shaanxi (Grant No. 2021JM-001).

†They contributed equally to this work.

*Corresponding authors. Email: zpantz@xjtu.edu.cn; huiyang.gou@hpstar.ac.cn

© 2021 Chinese Physical Society and IOP Publishing Ltd

magnetic moment collapse at high pressure. We further find that this site-dependent magnetic moment collapse originates from the energy level shifting and the consequent charge transfer among the five Fe-3d orbits in Fe_5O_6.

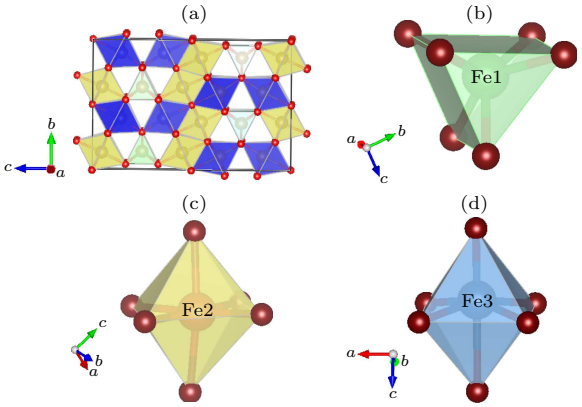

Fig. 1. Crystal structure of Fe_5O_6 (a) the FeO_6 trigonal prism at site-4c (Fe1) in green, (b) the FeO_6 octahedra at site-8$f1$ (Fe2) in yellow and (c) the FeO_6 octahedra at site-8$f2$ (Fe3) in blue.

In DFT + DMFT calculations, we adopt the Wien2k package[20] to derive the charge density, the eigenvector and the eigenenergy of crystal in DFT level. The Wu-Cohen[21] exchange-correlation potential with $20 \times 20 \times 4$ k-points is used. The exact double counting method[22] and the hybrid expansion continuous-time quantum Monte Carlo (CTQMC) method[23–25] are used to solve the self-consistent DMFT equation.[26] In each DMFT iteration, 10^7 Monte Carlo updates are used and the self-energy is derived from Dyson's equation. The converged self-energy from DMFT is used to update the new charge density and the new Kohn–Sham potential for the next DFT calculation. The DFT + DMFT loops iterate until the fully convergence of the charge density, the self-energy and the hybridization functions and so on. The maximum entropy method is used for analytic continuation of the self-energy from the imaginary frequency to the real frequency.[27]

We employ the constrained density functional theory method[28] to determine the screened Coulomb interaction U and Hund's coupling J among the Fe-3d electrons. In orthorhombic Fe_5O_6, there are three non-equivalent iron atoms: Fe1 (site-4c), Fe2 (site-8$f1$) and Fe3 (site-8$f2$). We derive the Coulomb U and Hund's J at $V_0 = 743.41\,\text{bohr}^3/Fe_5O_6$ and at $V = 698.34\,\text{bohr}^3/Fe_5O_6$ [at 11.4 GPa, also noted as $R = (1 - V/V_0)\% = 5.25\%$ representing the rate of volume compression]. At $V_0 = 743.41\,\text{bohr}^3/Fe_5O_6$ $(U, J) = (5.15\,\text{eV},\ 1.03\,\text{eV})$ at Fe1, $(5.08\,\text{eV},\ 0.97\,\text{eV})$ at Fe2, and $(4.62\,\text{eV},\ 0.97\,\text{eV})$ at Fe3. At 11.4 GPa, $(U, J) = (5.04\,\text{eV},\ 0.83\,\text{eV})$ at Fe1, $(5.02\,\text{eV},\ 0.87\,\text{eV})$ at Fe2, and $(4.45\,\text{eV},\ 0.95\,\text{eV})$ at Fe3. Since the value of the Coulomb interaction U and Hund's coupling J is not sensitive to the sites of iron atoms and the volume of Fe_5O_6 per unit cell, throughout our DFT + DMFT calculations we choose the average $(U, J) = (5.88\,\text{eV},\ 0.88\,\text{eV})$. DFT+$U$ volume optimization with $(U - J = 5.0\,\text{eV})$ predicts $V_0 = 743.41\,\text{bohr}^3/Fe_5O_6$ is the volume at the ambient pressure. In DFT + DMFT we further try $(U, J) = (5.88\,\text{eV},\ 1.0\,\text{eV})$, $(10.0\,\text{eV},\ 1.0\,\text{eV})$ and $(10.0\,\text{eV},\ 0.88\,\text{eV})$ under the ambient conditions and find that all of the conclusions in this study stay valid being independent of the specific values of U and J, as presented above.

It is known that under ambient conditions iron oxides such as FeO and Fe_2O_3 are insulators, while in contrast Fe_3O_4 is a metal. There is debate about the electronic conductibility of FeO_2.[29,30] Our DFT + DMFT calculations prove that Fe_5O_6 is a metal at the ambient pressure like Fe_3O_4. In Fig. 2, we present the total and the partial density of states (DOS) of Fe_5O_6. The total DOS of Fe_5O_6 has large quasi-particle peaks at the Fermi level in Fig. 2(a) at $743.41\,\text{bohr}^3/Fe_5O_6$ corresponding to the ambient pressure and in Fig. 2(b) at $408.88\,\text{bohr}^3/Fe_5O_6$ of 45% volume compression. This proves the metallic nature of Fe_5O_6 either at the ambient pressure or at high pressure. In addition, the height of quasi-particle peaks is relatively lower in Fig. 2(b) since the bandwidth of Fe_5O_6 is enlarged at high pressure. It is clearly shown in Figs. 2(c) and 2(d) that the total DOS of Fe_5O_6 at the Fermi level E_F is dominated by the Fe-3d bands, which suggests that the conductivity of Fe_5O_6 is mainly contributed by the Fe-3d electrons.

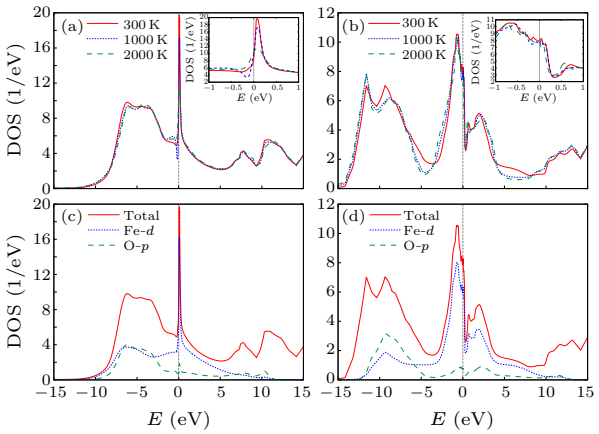

Fig. 2. The total density of states at 300 K, 1000 K, and 2000 K, (a) at the ambient pressure ($V_0 = 743.41\,\text{bohr}^3/Fe_5O_6$) and (b) at $R = 45\%$ volume compression ($V = 408.88\,\text{bohr}^3/Fe_5O_6$). The partial density of states of the Fe-3d orbits and the O-p orbits at 300 K (c) at the ambient pressure and (d) at 45% volume compression.

There will be a collapse of the magnetic moment in iron oxides at high pressure.[30–36] Our DFT + DMFT calculations of the local magnetic moment $\sqrt{\langle m_z^2 \rangle}$ indicate that there is site-selective magnetic moment collapse in Fe_5O_6 under compression. As shown in Fig. 3, when Fe_5O_6 is compressed, the local magnetic moment of Fe2 (8$f1$) decreases first, then the local magnetic moment of Fe3 (8$f2$), and the local magnetic

moment of Fe1 ($4c$) is the last to decrease. At the 45% volume compression endpoint, the magnetic moments of Fe2 ($8f1$) and Fe3 ($8f2$) saturate at about $0.8\mu_B$/Fe and $1.1\mu_B$/Fe, respectively, in contrast the magnetic moment of Fe1 ($4c$) ends at about $1.4\mu_B$/Fe. The dependence of the local magnetic moment on temperature and volume compression is summarized in the three diagrams in Fig. 4. It is clear that the magnetic moments of the three non-equivalent iron atoms always decrease as being compressed at any temperature from 300 K to 2000 K. Either at low temperature or at high temperature, the magnetic moment of Fe atoms collapses first at $8f1$ position, and then $8f2$ position, the last is at $4c$ position. In Fig. 4(a), 4(b) and 4(c), the green region that represents the magnetic moment of intermediate size expands as the temperature is increased, which indicates that decrement of the magnetic moment is slower at high temperature.

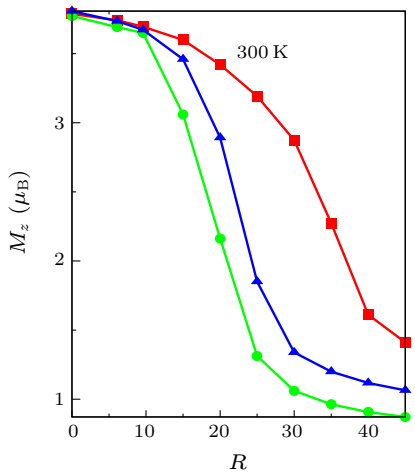

Fig. 3. The local magnetic moment of three non-equivalent iron atoms in Fe_5O_6 as a function of volume compression rate at 300 K. The red, the green, and the blue lines represent the local magnetic moments of Fe1 (site-$4c$), Fe2 (site-$8f1$), and Fe3 (site-$8f2$) respectively.

In transition metal oxides, the collapse of magnetic moment is often accompanied by the insulator-metal transition and the collapse of volume.[32–36] Thus, the insulator-metal transition is presumed to be related to the collapse of magnetic moment. However, in Fe_5O_6 we show the site-selective high spin-low spin transition of three iron atoms can be independent of the insulator-metal transition because Fe_5O_6 is always metallic, from ambient pressure to high pressure. Similar behavior has also been found in FeO_2.[30] This raises the question of whether or not the metallization of Mott insulator is the consequence of the pressure driven high spin-low spin transition.

It has been proven that the magnetic moment collapse in transition metal oxides such as FeO and MnO originates from the transfer of electrons among the d-orbits of the transition metals.[32–34,36] As shown in Fig. 5, we present the Fe-3d electron occupancies at Fe1 ($4c$), Fe2 ($8f1$) and Fe3 ($8f2$) of Fe_5O_6 at 300 K. When volume compression rate increases, the electron occupancies of the z^2, x^2-y^2 and xz orbits increase at all three crystallographic non-equivalent sites, while the electron occupancies of the yz and xy orbits decrease. This indicates that the charge transfer from the yz and xy orbits to the z^2, x^2-y^2 and xz orbits upon the volume compression. However, for Fe1 ($4c$), the charge transfer from the yz and xy orbits to the z^2 and xz orbits start at relatively larger volume compression rate R than that of Fe2 ($8f1$) and Fe3 ($8f2$), and the electron occupancy of the x^2-y^2 is almost constant until R is above 40%. This indicates that the electrons at Fe1 ($4c$) have stronger correlations than the electrons at Fe2 ($8f1$) and Fe3 ($8f2$). This electron transfer among the Fe-3d orbits is temperature dependent in that at higher temperature the charge will transfer at a lower rate.

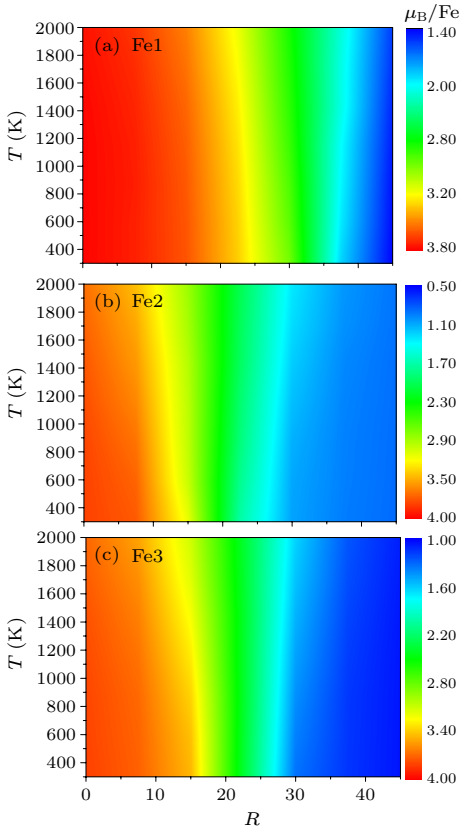

Fig. 4. The dependence of local magnetic moments on temperature and volume compression rate at the three non-equivalent positions of Fe_5O_6 (a) Fe1 (site-$4c$), (b) Fe2 (site-$8f1$), and (c) Fe3 (site-$8f2$).

The relationship between the local magnetic moment collapses of iron atoms and the charge transfer among the Fe-3d orbits could be understood at the atomic limit. At the low-pressure end, all five Fe-3d orbits have almost the same number of electrons and the magnetic moments is maximized at around $4.0\mu_B/Fe$ due to Hund's rule. At the high-pressure limit when the yz and the xy orbits have lost all of their electrons, the six electrons on the z^2, x^2-y^2 and xz orbits must form singlet pairs because of Pauli's exclusion principle, which leads to zero total magnetic

moment.

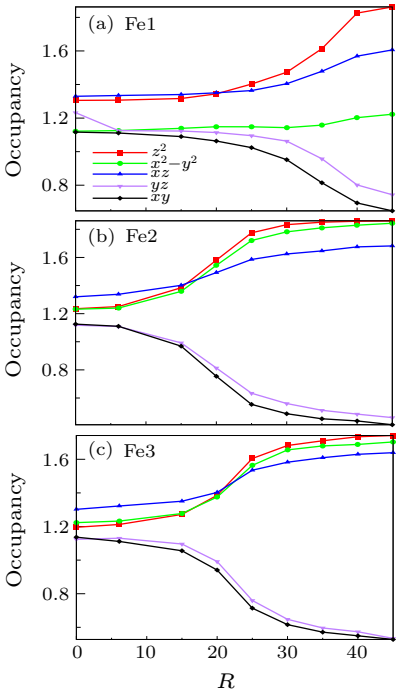

Fig. 5. The electron occupancy number of the Fe-3d orbits of atom (a) Fe1 (site-4c), (b) Fe2 (site-8$f1$) and (c) Fe3 (site-8$f2$) as a function of volume compression at 300 K.

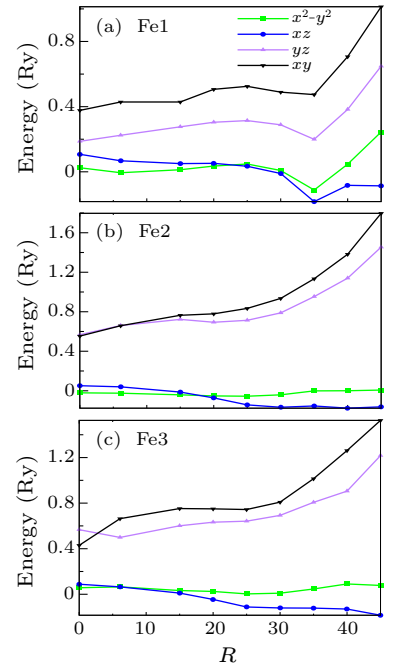

Fig. 6. The energy differences of the Fe-3d orbits of atom (a) Fe1 (site-4c), (b) Fe2 (site-8$f1$), and (c) Fe3 (site-8$f2$) as a function of volume compression rate at 300 K.

The transfer of electrons among the five Fe-3d orbits originates from the shift of energy levels of the Fe-3d orbits under compression. The energy difference of the x^2-y^2, xz, yz and xy orbits relative to the z^2 orbit under compression is shown in Fig. 6. In Figs. 6(b) and 6(c), upon compression energies of the yz and xy orbits at Fe2 (8$f1$) and Fe3 (8$f2$) sites moves upward; however, the energies of the x^2-y^2 orbits stay almost invariant and energy of xz even decrease. Then naturally electrons on the yz and xy orbits transfer to the z^2, x^2-y^2, and xz orbits to minimize the total energy in Fe_5O_6. In contrast, in Fig. 6(a), the orbital-energy differences of the yz and xy orbits of Fe1 (4c) increase much more slowly under compression, which leads to the slower magnetic moment collapse, as observed in Fig. 3.

In summary, we have examined the electromagnetic properties of the recently discovered iron oxides Fe_5O_6 under the high-pressure and high-temperature conditions of the Earth's interior by employing the DFT + DMFT method. Our calculations prove that paramagnetic Fe_5O_6 is metallic at ambient pressure and at high pressure. The electronic conduction in Fe_5O_6 is dominated by the Fe-3d electrons. The local magnetic moments of three crystallographic nonequivalent iron atoms in Fe_5O_6 collapse at different rates when being compressed, which leads to site-dependent magnetic moment collapse. We further find that the site-dependent magnetic moment collapse in Fe_5O_6 originates from the energy level shifting and the consequent charge transfer among the five Fe-3d bands under volume compression. Since Fe_5O_6 is a candidate component of the Earth's mantle beside the insulator FeO, the metallic nature of Fe_5O_6 suggests that the conductivity of the Earth's mantle could be higher than those previously expected. The electronic conductivity and the related thermal conductivity of the Earth's mantle may strongly affect the dynamics in Earth's deep interior. For example, they could determine the energy exchange rate and the mass distribution of Earth's low mantle-core boundary, which may induce anomalous features in seismic velocity. Thus, further investigations on Fe_5O_6 and other new iron oxides are called for to determine the precise value of the electronic conductivity and the thermal conductivity in the Earth's interior environment.

We thank the High Performance Computing platform of Xi'An Jiaotong University for providing the allocation of CPU time.

References

[1] Crane R A and Scott T B 2013 *J. Nanotechnol.* **10** 1155
[2] Cornell R M and Schwertmann U 2004 *The Iron Oxides: Structure, Properties, Reactions, Occurences and Uses* 2nd edn (New York: Wiley-VCH Verlag)
[3] Wood B J, Bryndzia L T and Johnson K E 1990 *Science* **248** 337
[4] Cornell R M and Schwertmann U 2004 *The Iron Oxides: Structure, Properties, Reactions, Occurences and Uses* 2nd edn (New York: Wiley-VCH Verlag) p 1
[5] Rosales S, Casillas N, Topete A, Cervantes O, Gonzalez G, Paz J A and Cano M E 2020 *Chin. Phys. B* **29** 100502
[6] Hua L Z, Xiang L and Wei L 2019 *Chin. Phys. B* **28** 077504
[7] Yu W Q, Qiu Y C, Xiao H J, Yang H T and Wang G M 2019 *Chin. Phys. B* **28** 108103

[8] Wenjun Y, Xiaomin Z, Huan L, Chunwei G, Min L and Houpan Z 2019 *Chin. Phys. B* **28** 106801
[9] Yang Y, Zhang Q, Mi W and Zhang X 2020 *Chin. Phys. B* **29** 083302
[10] Hu Q Y, Kim D Y, Yang W G, Yang L X and Meng Y 2016 *Nature* **534** 241
[11] Nishi M, Kuwayama Y, Tsuchiya J and Tsuchiya T 2017 *Nature* **547** 205
[12] Lavina B, Dera P, Kim E, Meng Y and Downs R T 2011 *Proc. Natl. Acad. Sci. USA* **108** 17281
[13] Lavina B and Meng Y 2015 *Sci. Adv.* **1** e1400260
[14] Zhang X L, Niu Z W, Tang M, Zhao J Z and Cai L C 2017 *J. Alloys Compd.* **719** 42
[15] Sinmyo R, Bykova E, Ovsyannikov S V, McCammon C and Kupenko I 2016 *Sci. Rep.* **6** 32852
[16] Merlini M, Hanfland M, Salamat A, Petitgirard S and Müller H 2015 *Am. Mineral.* **100** 2001
[17] Koutaro H, Ryosuke S, Kei H, Takayuki I and Yasuo O 2019 *Am. Mineral.* **104** 1356
[18] Ovsyannikov S V, Maxim B, Medvedev S A and Naumov P G 2020 *Angew. Chem.* **59** 5632
[19] Kotliar G 2006 *Rev. Mod. Phys.* **78** 865
[20] Blaha P, Schwarz K, Madsen G K H, Kvasnick K and Luitz J 2001 *Wien2K* ed Schwarz K (Technische Universitat Wien)
[21] Wu Z G and Cohen R E 2006 *Phys. Rev. B* **73** 235116
[22] Haule K 2015 *Phys. Rev. Lett.* **115** 196403
[23] Gull E, Millis A J, Lichtenstein A I, Rubtsov A N, Troyer M and Werner P 2011 *Rev. Mod. Phys.* **83** 349
[24] Werner P, Comanac A and de'Medici L 2006 *Phys. Rev. Lett.* **97** 076405
[25] Haule K 2007 *Phys. Rev. B* **75** 155113
[26] Georges A, Kotliar G, Krauth W and Rozenberg M J 1996 *Rev. Mod. Phys.* **68** 13
[27] Madsen G K H and Novak P 2005 *Europhys. Lett.* **69** 777
[28] Jarrell M and Gubernatis J E 1996 *Phys. Rep.* **269** 133
[29] Bo G J, Kim D Y and Ji H S 2017 *Phys. Rev. B* **95** 075144
[30] Koemets E 2021 *Phys. Rev. Lett.* **126** 106001
[31] Cohen R E, Mazin I I and Isaak D G 1997 *Science* **275** 654
[32] Eran G 2018 *Phys. Rev. X* **8** 031059
[33] Kunes J, Korotin D M, Korotin M A, Anisimov V I and Werner P 2009 *Phys. Rev. Lett.* **102** 146402
[34] Kunes J, Lukoyanov A V, Anisimov V I, Scalettar R T and Pickett W E 2008 *Nat. Mater.* **7** 198
[35] Ohta K, Cohen R E, Hirose K, Haule K, Shimizu K and Ohishi Y 2012 *Phys. Rev. Lett.* **108** 026403
[36] Leonov I 2015 *Phys. Rev. B* **92** 085142